*Progress In Electromagnetics Research M, Vol. 69, 1–13, 2018*

# Frequency Reconfigurable Patch Antenna for 4G LTE Applications

**Hassan T. Chattha[1, 3], Maria Hanif[2, 3], Xiaodong Yang[4, *], Inam E. Rana[3], and Qammer H. Abbasi[5]**

**Abstract**—A compact printed multi-band frequency reconfigurable patch antenna for 4G LTE applications is presented in this paper ($50 \times 60 \times 1.6\,\text{mm}^3$). The antenna consists of W-shaped and Inverted-U shaped patch lines connected in a Tree-shape on the front side of the antenna. The back-side of the antenna contains a 90°-tilted T-shaped strip connected with an Inverted-L shaped strip which is shorted with a patch on the front side for increasing the electrical length to cover lower frequency bands. Frequency reconfigurability is achieved by inserting three switches i.e., PIN diodes. The most critical part of this work is the designing of RLC-based DC line circuits for providing the DC biasing to the PIN diodes used as switches and inserting them at optimum locations. This antenna is reconfigurable among eight different 4G LTE frequency bands including 0.9 GHz, 1.4 GHz, 1.5 GHz, 1.6 GHz, 1.7 GHz, 1.8 GHz, 2.6 GHz, 3.5 GHz and WLAN band 2.5 GHz. The antenna exhibits different radiation patterns having a different direction of peak gain at different frequencies and for different switching combinations. The antenna is simulated with CST, and a prototype is fabricated to compare the measured and simulated results with good accuracy.

## 1. INTRODUCTION

With the enhancement in the world of wireless communications, the need for multipurpose devices has increased. This need can be fulfilled with reconfigurable antennas [1]. Reconfigurability can be achieved in different categories like frequency, polarization and radiation pattern reconfigurations [2, 3]. This change is obtained by redistributing the antenna currents, thus, altering the electromagnetic fields of the antenna's effective aperture. Regarding the adjustable parameters of the antennas, reconfigurable antennas can be divided into many sub-categories which include frequency reconfigurable antenna, pattern reconfigurable antenna, polarization reconfigurable antenna, frequency-polarization hybrid reconfigurable antenna and frequency-pattern hybrid reconfigurable antenna among which frequency reconfigurable antennas are found more in the literature [4–6].

There are different techniques used for making the antenna reconfigurable. One of the techniques is the addition of an electrical device like RF MEMS, PIN diodes and the varactors. Other techniques include photoconductive (optical), physical structural alteration and use of materials like liquid crystal and ferrites [3]. In literature, numerous reconfigurable antennas are found using these different techniques. In [7], pin diodes were used to cover the 5.25 and 5.75 GHz portion of the wireless LAN spectrum. The authors in [8] incorporated three PIN diodes to cover Wi-Fi and WiMAX portion of the electromagnetic spectrum. In [9], they designed a reconfigurable microstrip antenna for the frequency bands of 2.4 GHz and 5.6 GHz having RF PIN diodes inserted as switches. A circular patch microstrip feed reconfigurable antenna for WLAN wireless communications was presented in [10]. In [11], the

*Received 21 February 2018, Accepted 25 April 2018, Scheduled 23 May 2018*

* Corresponding author: Xiaodong Yang (xdyang@xidian.edu.cn).

[1] Department of Electrical Engineering, Faculty of Engineering, Islamic University of Madinah, Al-Madinah, Saudi Arabia. [2] Department of Electrical Engineering, GC University, Faisalabad, Pakistan. [3] Department of Electrical Engineering, University of Engineering & Technology, Lahore, Pakistan. [4] School of Electronic Engineering, Xidian University, Xi'an, Shaanxi 710071, China. [5] School of Engineering, University of Glasgow, Glasgow G12, 8QQ, UK.

authors designed a reconfigurable UWB antenna and incorporated it with RF-MEMS which made it capable of on-demand WLAN rejection. An antenna aware of its surroundings by incorporating IR sensors was presented in [12]. A miniaturized antenna for multi-radio wireless communication was presented in [13] which used PIN diodes for achieving reconfigurability. [14] presented a reconfigurable antenna for wireless temperature sensing. In [15], the authors presented an antenna capable of working between 2.4–2.57 GHz which can switch its polarization from left-hand to right-hand circular polarizations and vice versa. A frequency reconfigurable antenna covering LTE bands having MIMO capabilities was presented in [16]. Antenna presented in [17] works between 2–3.2 GHz and achieves reconfigurability by using RF MEMS switches. The design and analysis of an RF MEMS based reconfigurable antenna for use in the United States public safety bands are presented in [18]. [19] presented a small RF MEMS switched planar Inverted-F antenna capable of operation in five cellular radio frequency bands. The authors in [20] presented a reconfigurable PIFA using a switchable PIN diode and a fine-tuning varactor for USPCS (1.85–1.99 GHz), WCDMA (1.92–2.18 GHz), and WLAN (5.15–5.825 GHz) bands. In [21], the authors presented a varactor diode based reconfigurable mobile antenna covering a frequency band between 1.7 GHz and 2.4 GHz. A reconfigurable patch antenna possessing an E-shaped structure is presented in [22] where the operation frequency is changed by integrating switches. Ali et al. developed four reconfigurable antenna elements, including the Yagi, the corner-fed triangular loop, center-fed equilateral triangular loop and rectangular spiral reconfigurable antennas to work at 2.45 GHz and 5.78 GHz bands [23]. A frequency reconfigurable patch antenna, by applying the Finite-Difference Time-Domain method, was presented in [24]. [25] presented an annular slot antenna using PIN diodes to reconfigure the impedance match and modify the radiation pattern of the antenna. Optically controlled frequency reconfigurable microstrip antennas are presented in [26, 27]. A microstrip patch antenna operating in 5 GHz range is presented in [28] where tuning was achieved using liquid crystal. [29] presented a circular beam steering reconfigurable antenna with liquid metal parasitics. The variation in the height and the angular position of the ground plane was exploited to tune the frequency response of a reconfigurable antenna presented in [30]. In some papers found in literature, the reconfigurable antennas are presented in which the switches are assumed 'ON' and 'OFF' only in simulations by replacing the diodes (used as switches) with their equivalent circuits values of resistance, capacitance and/or inductor in their 'ON' and 'OFF' states and just showing the simulated results, and no DC biasing mechanism is provided for changing the states of the switches physically or electronically. In [31–33], the authors have presented reconfigurable multi-band printed monopole antennas for different wireless applications. However, they have assumed switches 'ON' and 'OFF' only in simulations and have presented simulated results only. Similarly, the authors in [34] have proposed a microstrip-fed planar antenna covering four different frequency bands including 900 MHz, 1.8 GHz, 2.4 GHz and 3.5 GHz. The three switches, added for reconfigurability, are assumed in 'ON' and 'OFF' states in simulations only and the results of simulations are presented in tabular form only with no DC biasing mechanism for changing the states of the switches. A similar situation is found in [35, 36] where frequency reconfigurable planar Inverted-F antennas are proposed for different wireless applications.

In this paper, we have proposed a reconfigurable printed patch antenna capable of communication over eight different 4G LTE bands. The reconfigurability in this patch antenna is achieved using three RF PIN diodes as switches. PIN diodes are the devices having high switching capabilities and can be made to act as a short circuit, an open circuit or exhibiting any desired reflection coefficient in between [37]. Control of active components, i.e., PIN diodes, is the main and critical part of this reconfigurable antenna. These switches are controlled by three separate DC lines. But as DC lines are also conducting elements, they interrupt the path of current, so to cut them from radiating part of the antenna, the inductors are added in DC lines. The capacitors are inserted between the DC sources and the ground plane to avoid the flow of DC current to the ground.

The paper is organized as follows: Section 2 describes the antenna design configurations, and Section 3 explains the DC biasing of the PIN diodes used as switches. Section 4 discusses and compares the results of reflections coefficients and radiation patterns achieved through simulations and measurements whereas Section 5 shows the current distributions on different patches of the antenna at different frequencies to get an insight and the behavior of these patches at working frequencies.

## 2. ANTENNA DESIGN CONFIGURATION

The top view of the proposed antenna is shown in Fig. 1 having a compact dimension of $50\times60\times1.6\,\text{mm}^3$. The front/top side of the antenna consists of five patches. These front-side patches are placed in a W-shaped and Inverted-U shaped structure giving a look of a tree. The proposed antenna is designed on a substrate of material FR4 having a dielectric constant of 4.4 and thickness of 1.6 mm with a copper layer of thickness 0.1 mm. To make the proposed antenna work for different 4G LTE bands, we need to change the current densities and the electrical length of the antenna. For this purpose, three RF silicon PIN diodes to work as switches are inserted in the antenna structure as shown in Fig. 1. The silicon PIN diodes used as switches have the model BAR64 by Infineon Technologies with a working frequency range from 1 MHz to 6 GHz. For simulation purposes, we need to see its equivalent circuits in 'ON' and 'OFF' states. This diode has a very low forward resistance of 2.0 Ω in forward biased condition and a parallel combination of resistance 3 KΩ and a capacitance of 0.17 pF in reverse biased condition. These values are used in the simulations of this antenna design in 'ON' and 'OFF' states of the PIN diode used as a switch. The three PIN diodes used as switches are named as Switch 1, Switch 2 and Switch 3. Switch 1 is placed between Patch 1 and Patch 2. Switch 2 is placed between Patch 2 and Patch 3 whereas Switch 3 is placed between Patch 4 and Patch 5 as shown in Fig. 1. By switching these diodes 'ON' and 'OFF', the antenna achieves reconfigurability. In order to operate/activate these diodes, DC biasing is needed. For this purpose, three DC lines are added in the antenna design which is explained in the next section. The width of all the patches on the front and the back sides is the same and is equal to $W_{SP} = 3.5\,\text{mm}$. The vertical lengths of Patches 1, 2, 3, 4 and 5 are $L_{s4}$, $L_{s3}$, $L_{s2}$, $L_{s5}$ and $L_{s1}$ respectively. The horizontal length of Patch 4 is $L_{s12}$ whereas that of Patch 5 is $L_{s6}$. The vertical heights of the Patch 1, Patch 3 and Patch 5 from the bottom end of the antenna are $H_1$, $H_2$ and $H_3$ respectively. The detailed dimensions of the front side of the antenna are shown in Table 1. The bottom side of the antenna also contains two patches and a ground plane as shown in Fig. 2. One of the patches placed on the back side of the antenna has a 90°-tilted T-shaped structure connected with the patch having an Inverted-L shaped structure which is shorted with Patch 5 on the front side through the substrate. The vertical and horizontal lengths of the T-shaped patch are $L_{s7} = 40\,\text{mm}$ and $L_{s10} = 45\,\text{mm}$ respectively. Similarly, the vertical and horizontal lengths of the L-shaped patch are $L_{s8} = 19\,\text{mm}$ and $L_{s9} = 31.5\,\text{mm}$ respectively. The inverted-L shaped patch is connected to the T-shaped patch at a distance $L_{s11} = 12.8\,\text{mm}$. The width of these two patches on the back side is also the same as that of in the front side and is equal to $W_{SP} = 3.5\,\text{mm}$. The ground plane dimensions of this antenna are much smaller than the overall dimensions of the antenna and are equal to $L_w \times G_w$ $(10.5 \times 50\,\text{mm}^2)$.

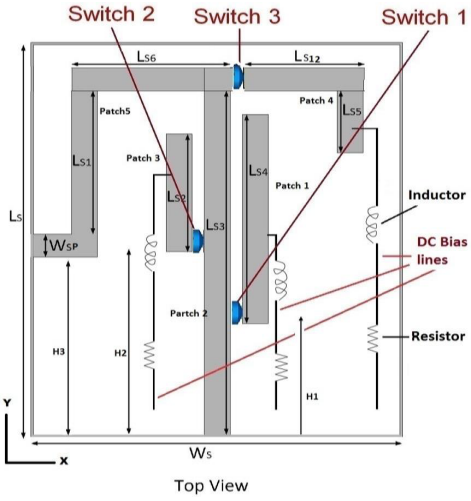


**Figure 1.** Top view of the proposed reconfigurable patch antenna.

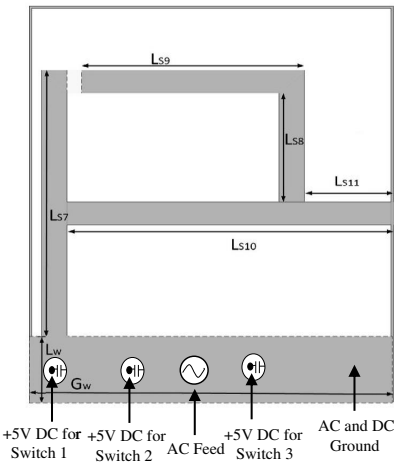


**Figure 2.** Bottom view of the proposed reconfigurable patch antenna.

**Table 1.** Antenna dimensions.

| Parameters | Dimensions (mm) | Parameters | Dimensions (mm) |
|---|---|---|---|
| $W_s$ | 50 | $L_{s6}$ | 21.75 |
| $L_s$ | 60 | $L_{s12}$ | 16.45 |
| $L_{s1}$ | 25.5 | $H_1$ | 17.5 |
| $L_{s2}$ | 18 | $H_2$ | 28 |
| $L_{s3}$ | 53 | $H_3$ | 27.5 |
| $L_{s4}$ | 32 | $W_{sp}$ | 3.5 |
| $L_{s5}$ | 13 | | |

## 3. DC BIASING

For the proposed antenna to be reconfigurable, the silicon PIN diodes are used as switches. However, the PIN diode needs a DC input for activation, whereas the antenna works on an AC input.

For DC biasing of the PIN diodes, three $\lambda/4$ DC lines are added in the antenna structure as shown in Fig. 1. The lengths of these $\lambda/4$ lines are calculated through the use of microstrip transmission line theory [38]. For example, using microstrip transmission line theory, the $\lambda/4$ length of the DC line connected to Patch 1 comes equal to around 27 mm corresponding to the relative permittivity of the substrate $\varepsilon_r = 4.4$, width of patch $W_{sa} = 3.5$ mm, height of substrate $t = 1.6$ mm and the length of patch $L_{s4} = 34$ mm. Similarly, for Patches 3 and 4, the corresponding lengths of $\lambda/4$ DC lines are found equal to be around 34 mm and 38 mm respectively. To select the position of connection of DC line with the corresponding patch, the current distribution at different frequencies is observed on the respective patch, and the connection point is selected where current is found minimum on the patch, so that it minimally affects the flow of AC current on the patch and to reduce the AC current flow through the DC line.

However, the presence of DC lines disturbs the flow of AC current and provide an alternative path to the flow of AC current. So, to avoid the AC current to flow through the DC lines, the inductors need to be inserted in the path of DC lines. As inductors work as RF chock which stops AC current from flowing. The value of the inductor is calculated per the minimum operating frequency of the antenna. Since the minimum operating frequency of the antenna is 0.9 GHz and above, we can safely assume the value of 0.8 GHz for calculating the value of inductors to be used in each DC line. Since the inductor impedance should be high to avoid the flow of AC current, the value of inductor impedance should be greater than 500, i.e., $X_L \geq 500$. So

$$\begin{aligned} X_L &= 2\pi f L \\ L &= \frac{X_L}{2\pi f} \\ L &= \frac{500}{2 \times \pi \times 0.8 \times 10^9} = 99.5\,\text{nH} \end{aligned} \tag{1}$$

A resistor of 1 KΩ is inserted in the DC line to control the flow of DC current. The circuit schematic of a DC line is shown in Fig. 3. As shown in Fig. 3, it contains a capacitor between the +5-volt DC source and the ground. The insertion of a capacitor serves two purposes; it blocks the DC current to flow to the ground, and it acts as a short circuit for AC current and thus stopping AC current from flowing through the DC source. Since the capacitor is serving as an AC short-circuit, its impedance is assumed as low as 1 Ω. And, like the inductor case, the value of frequency is taken as 0.8 GHz. So

$$X_C = \frac{1}{2\pi f C}$$

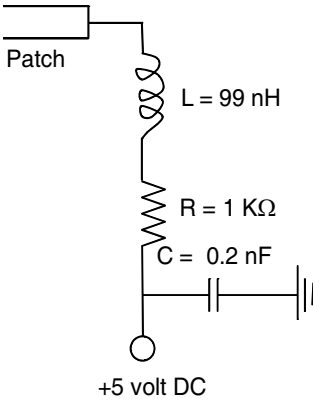


**Figure 3.** The circuit schematic of the DC line.

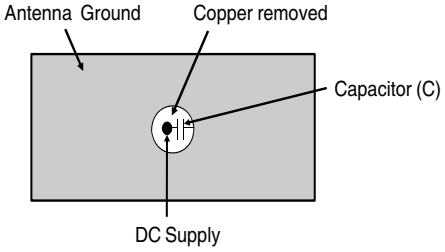


**Figure 4.** The physical mechanism used to connect DC supply through the ground plane.

$$C = \frac{1}{2\pi f X_C}$$
$$C = \left(\frac{1}{2 \times 3.14 \times 0.8 \times 10^9}\right) = 0.2\,\text{nF} \quad (2)$$

As shown in Fig. 1, one end of the DC lines is shorted to the patches whereas the DC source is connected to the other end of the DC lines through the substrate as shown in Fig. 2. As can be seen in Fig. 2, three DC sources are connected on the bottom side of the antenna by removing/etching small circular slots in the ground plane. To stop the DC current from flowing to the ground, a capacitor of 0.2 nF, calculated above, is inserted between the DC source and the ground plane. Fig. 4 clearly highlights the physical mechanism used to connect a DC supply to the DC line through the ground plane. The proposed antenna is simulated in CST Microwave Studio v. 12.

## 4. RESULTS AND DISCUSSION

For measurement purposes, a prototype of the proposed reconfigurable antenna is fabricated as shown in Fig. 5. Instead of using one inductor of 99 nH, three surface mount inductors of 33 nH each are inserted at an equal distance from each other in each DC line. The measurement setup used to measure the

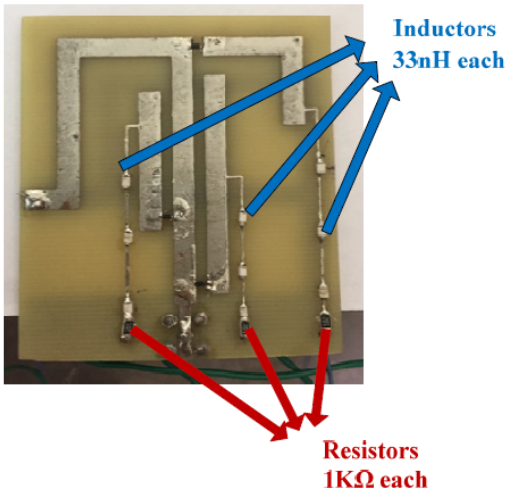


**Figure 5.** A fabricated prototype of the reconfigurable antenna.

**Table 2.** Frequency bands covered by different switching combinations.

| Switching Modes | Frequency Bands Covered (GHz) | | |
|---|---|---|---|
| Case 1 (000) | 2.5 | 2.6 | |
| Case 2 (001) | 1.4 | 1.8 | 2.6 |
| Case 3 (011) | 1.7 | 2.6 | |
| Case 4 (100) | 1.5 | 1.6 | |
| Case 5 (101) | 0.9 | 1.5, 1.6, 1.7 | 2.6 |
| Case 6 (110) | 1.5 | 1.6 | 3.5 |
| Case 7 (111) | 1.5 | 1.6 | 2.6 |

reflection coefficient $S_{11}$ in dB consists of a Keysight FieldFox (N9916A) Microwave Network Analyzer having a frequency range of up to 14 GHz and three DC supplies.

As three PIN diodes are used as switches in this reconfigurable antenna, there are eight possible combinations depending on the 'ON' and 'OFF' state of each PIN diode used as a switch. In this paper, we present the results of all the possible combinations except for only one combination where the results are not in any of the required bands. The switches are numbered as shown in Fig. 1. The cases/modes presented in this paper in binary numbers are 000, 001, 011, 100, 101, 110, and 111 where 0 means the switch is in 'OFF' state, and 1 means the switch is in 'ON' state. The state of Switch 1 is presented by the binary number on the right in the combination, and middle binary number presents the state of Switch 2, whereas the state of Switch 3 is presented by the binary number on the left in the combination. Table 2 shows all the cases presented in this paper along with the frequency bands covered corresponding to the different switching modes. Some frequency bands are covered by different states. It is because we want to have different frequency combinations from which we can select the frequency combination as per requirement/demand. For example, as shown in Table 2, the 2.6 GHz band is covered by states 000, 001, 011, 101 and 111 along with different frequency bands, but it is not at all covered by states 100 and 110. Therefore, as per requirement, the 2.6 GHz can be chosen with different frequency bands, and if required, it can be avoided by selecting the states where it is not at all covered.

Reflection coefficients $S_{11}$ for all the presented cases are measured and compared with the simulated ones described as follows which are found generally in good agreement where small variations are attributed to manufacturing tolerance.

### 4.1. Case 1 (000)

The first case presents the situation where all the switches are in 'OFF' states. The simulated and measured results of the reflection coefficient $S_{11}$ in dB are shown in Fig. 6. From the results, it is obvious that the proposed antenna covers 2.5 GHz WLAN band and 2.6 GHz LTE band for our criteria of $S_{11} < -10$ dB. The result shows that the antenna structure also resonates in the 3 GHz band; however, it does not come in our bands of interest.

### 4.2. Case 2 (001)

Case 2 presents the situation when Switch 2 and Switch 3 are in 'OFF' states and the Switch 1 is in 'ON' state. The simulated and measured results of reflection coefficient $S_{11}$ in dB are shown in Fig. 7. From the results, the proposed antenna covers 1.4 GHz, 1.8 GHz, and 2.6 GHz LTE bands.

### 4.3. Case 3 (011)

Case 3 presents the situation when Switch 1 and Switch 2 are in 'ON' states and switch 3 in 'OFF' state. The simulated and measured results of reflection coefficient $S_{11}$ are shown in Fig. 8. From the results, the proposed antenna covers 1.7 GHz and 2.6 GHz LTE bands.

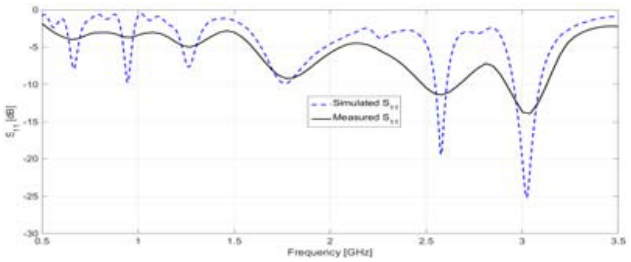


**Figure 6.** Measured and simulated reflection coefficient $S_{11}$ when all the switches are 'OFF' (000).

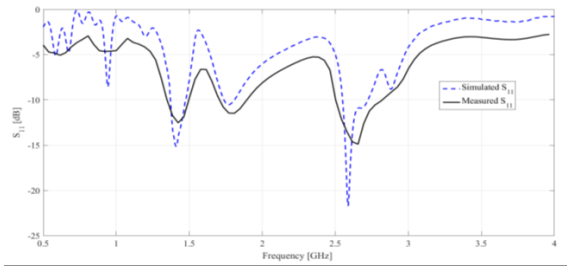


**Figure 7.** Measured and simulated reflection coefficient $S_{11}$ when only Switch 1 is 'ON' (001).

### 4.4. Case 4 (100)

Case 4 presents the situation when Switch 1 and switch 2 are in 'OFF' states and Switch 3 in 'ON' state. The simulated and measured results of reflection coefficient are shown in Fig. 9. From the results, the proposed antenna covers only 1.5 GHz and 1.6 GHz LTE bands.

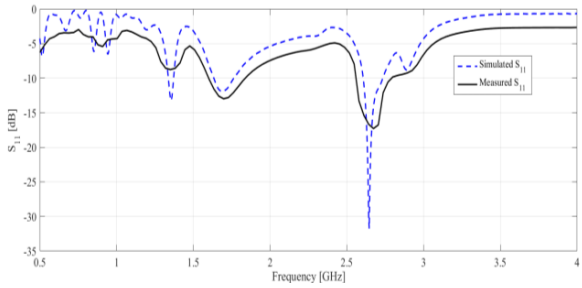


**Figure 8.** Measured and simulated reflection coefficient $S_{11}$ when only Switch 3 is 'OFF' (011).

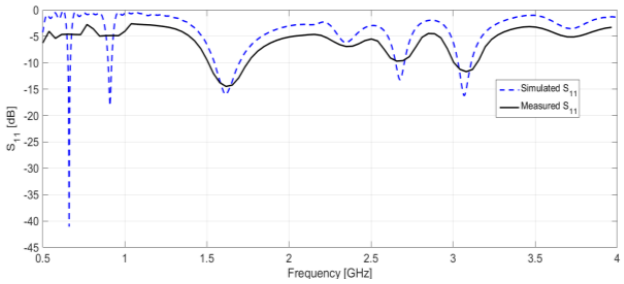


**Figure 9.** Measured and simulated reflection coefficient $S_{11}$ when only Switch 3 is 'ON' (100).

### 4.5. Case 5 (101)

Case 5 presents the situation when Switch 1 and Switch 3 are 'ON', and Switch 2 is 'OFF'. The simulated and measured results of reflection coefficient are shown in Fig. 10. From the results, the proposed antenna covers 0.9 GHz, 1.6 GHz, and 2.6 GHz LTE bands.

### 4.6. Case 6 (110)

Case 6 presents the situation when Switch 1 is 'OFF', and Switches 2 and 3 are in 'OFF' states. The simulated and measured results of reflection coefficient are shown in Fig. 11. From the results, the proposed antenna covers 1.5 GHz, 1.6 GHz, and 3.5 GHz LTE bands.

### 4.7. Case 7 (111)

Case 7 presents the situation where all the switches are in 'ON' states. The simulated and measured results of reflection coefficient are shown in Fig. 12. From the results, the proposed antenna covers 1.5 GHz, 1.6 GHz, and 2.6 GHz LTE bands.

It is clear from the above-mentioned results of reflection coefficients for $S_{11} < -10$ dB that this reconfigurable antenna covers nine different LTE/WLAN frequency bands including 0.9 GHz, 1.4 GHz, 1.5 GHz, 1.6 GHz, 1.7 GHz, 1.8 GHz, 2.5 GHz, 2.6 GHz, and 3.5 GHz bands under different switching combinations/modes.

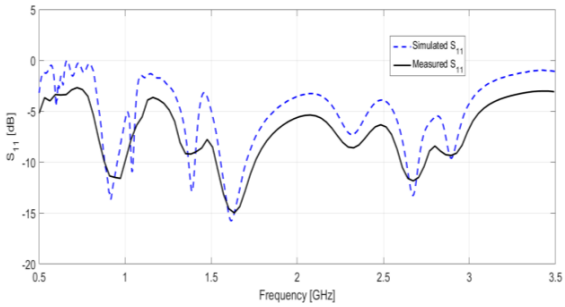


**Figure 10.** Measured and simulated reflection coefficient $S_{11}$ when only Switch 2 is 'OFF' (101).

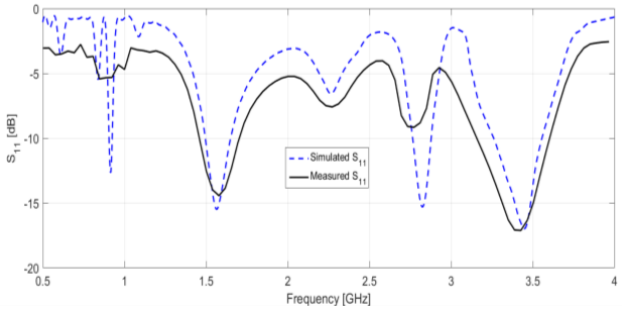


**Figure 11.** Measured and simulated reflection coefficient $S_{11}$ when only Switch 1 is 'OFF' (110).

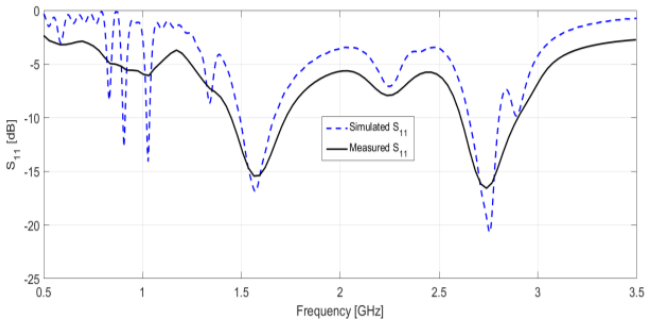


**Figure 12.** Measured and simulated reflection coefficient $S_{11}$ when all the switches are 'ON' (111).

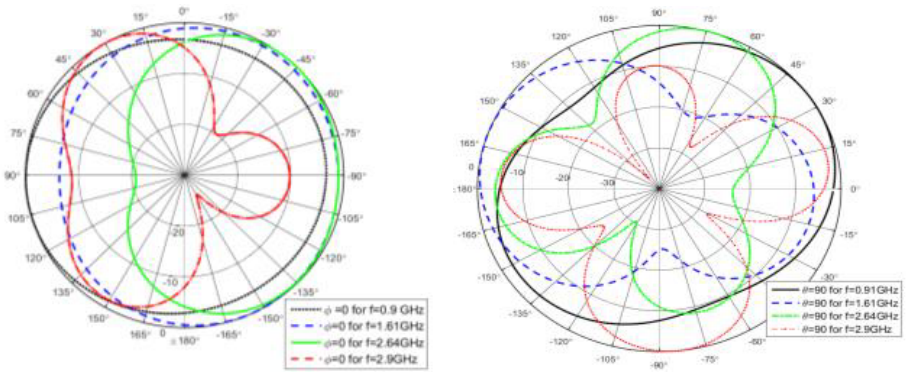


(a) (b)

**Figure 13.** 2D radiation patterns at different frequencies when only Switch 2 is 'OFF' (101) for (a) $XZ$ ($\Phi = 0°$) plane (b) $XY$ ($\theta = 90°$) plane.

To see pattern variations, we need to check the radiation patterns of this antenna at different frequency bands to see the pattern changes under different switching combinations.

First, we take the case of 101, when Switch 1 and Switch 3 are 'ON', and Switch 2 is in 'OFF' state. Fig. 13 shows the normalized 2D radiation patterns of this antenna in dB for $XZ$ ($\Phi = 0°$) and $XY$ ($\theta = 90°$) planes at frequencies 0.91 GHz, 1.61 GHz, 2.64 GHz, and 2.9 GHz. It can be seen that radiation patterns are quite different from each other at each frequency band. This is because different patches on the front and bottom sides are excited to produce resonance at these different bands which produce different radiation patterns.

To further elaborate the pattern changes/variations, Fig. 14 shows the 3D radiation patterns in

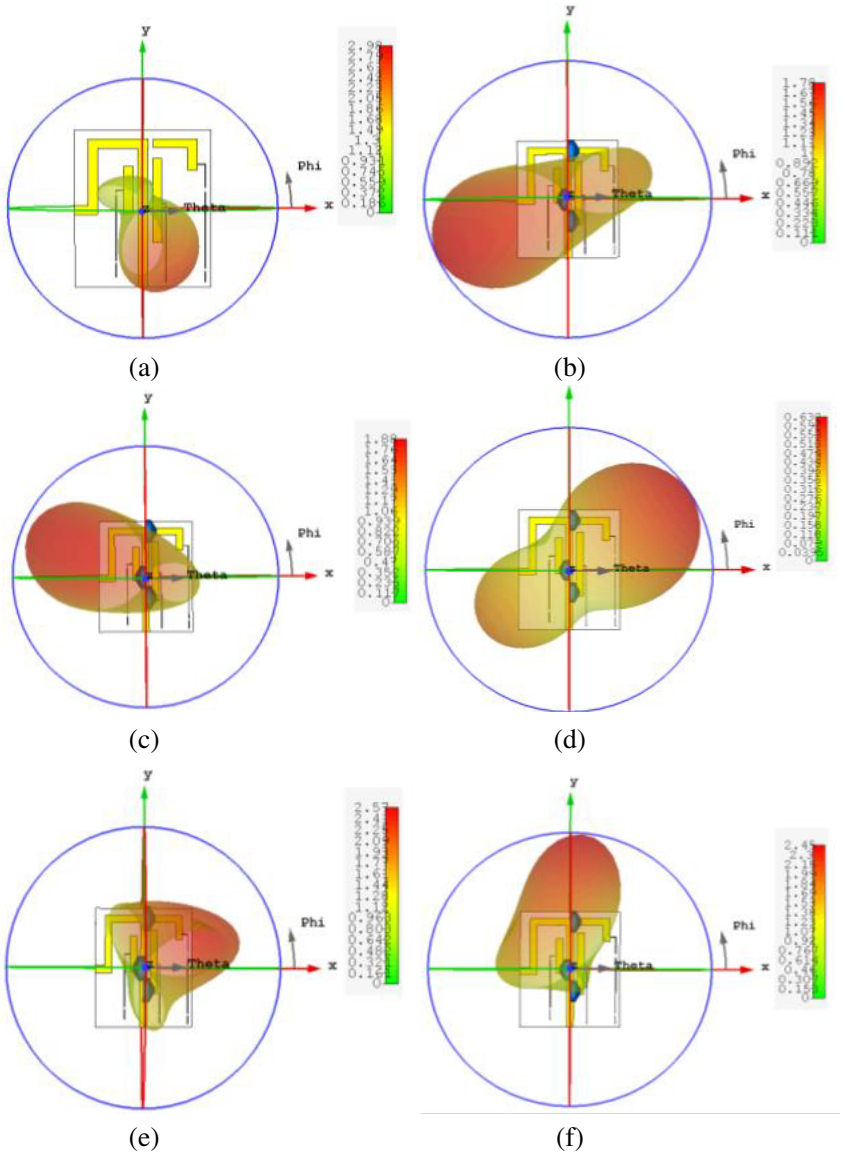


**Figure 14.** 3D radiation pattern of reconfigurable antenna at different frequencies under different switching combinations/cases. (a) 2.64 GHz for case 1 (000), (b) 1.4 GHz for case 2 (001), (c) 1.7 GHz for case 3 (011), (d) 0.91 GHz for case 5 (101), (e) 3.4 GHz for case 6 (110) (f) 2.6 GHz for case 7 (111).

linear scale at different frequencies under different switching combinations. Fig. 14(a) shows the 3D radiation pattern at 2.64 GHz for case 1 (000) when all the switches are 'OFF' and depicts that the pattern at this frequency is mainly directed towards around $\Phi = 270°$, and the peak gain found is 4.742 dBi. The 3D radiation pattern at 1.4 GHz for case 2 (001) when only Switch 1 is 'ON', and Switches 2 and 3 are 'OFF' is mainly directed towards around $\Phi = 210°$ as shown in Fig. 14(b) with the peak gain of 2.293 dBi. At 1.7 GHz for case 3 (011) when only Switch 3 is 'OFF', the 3D radiation pattern is mainly directed towards around $\Phi = 160°$ having a peak gain of 2.912 dBi as shown in Fig. 14(c). For case 5 (101) when only Switch 2 is 'OFF', and Switches 1 and 3 are 'ON', the 3D radiation pattern at 0.91 GHz is found mainly directed towards around $\Phi = 40°$ having a peak gain of 2.29 dBi as shown in Fig. 14(d). Fig. 14(e) shows the 3D radiation pattern at 3.4 GHz for case 6 (110) when only Switch 1 is 'OFF', and Switches 1 and 2 are 'ON' and depicts that the pattern at this frequency is mainly directed towards around $\Phi = 30°$, and the peak gain found is 4.097 dBi. At 2.6 GHz for case 7 (111) when all the switches are 'ON', the 3D radiation pattern is mainly directed towards around $\Phi = 90°$ having a peak

gain of 3.899 dBi as shown in Fig. 14(f). It is also evident from Figs. 13 and 14 that since the antenna is lying on $XY$ plane, it has directed beams with respect to $\Phi$ whereas it has isotropic or omnidirectional radiation patterns with respect to $\theta$. It is concluded that the radiation patterns at different frequencies under different switching combinations are quite different from each other which can be exploited in a future work to get pattern diversity in which different radiation patterns are achieved for different switching combinations. From Fig. 14, it is also evident that the higher the frequency is, the higher the peak gain would be, which will be explained in the next section.

## 5. DESIGN THEORY AND CURRENT DISTRIBUTIONS

Now the questions arise: How does this antenna cover different frequency bands under different switching combinations? How does this antenna produce different radiation patterns at different frequencies? And what is the reason that a higher resonant frequency achieves high peak gain? To answer these questions, we take help from the theory of monopole antennas [39]. We know that for a monopole antenna to produce resonance, its length should be equal to $\lambda/4$ where $\lambda$ is the wavelength corresponding to the resonant frequency. Since this reconfigurable antenna consists of considered like monopole antennas. Therefore, for the patch/patches to produce resonance at a typical frequency, its length should be equal to $\lambda/4$ where $\lambda$ is derived from that typical frequency. Therefore, the lower the frequency is, the higher should be the length of the patch to make it equal to $\lambda/4$ for producing resonance at that frequency. This justifies the extension of patches on the bottom side of the antenna to increase the electrical length of the antenna to produce resonance at lower frequency bands such as 0.9 GHz. So, for different switching combinations, different patches come into the circuit which produces resonance when their electrical length becomes equal to $\lambda/4$ corresponding to the resonant frequency. Since under different switching combinations, different patches having different lengths come into the circuit, it produces different radiation patterns as the current distribution is different for different switching combinations/cases. As the length required to produce resonance at lower frequency is higher such as at 0.9 GHz, the current is distributed on both sides (top and bottom) of the antenna and on both left and right hand sides of the feeding middle patch (Patch 2), which produces relatively omnidirectional radiation pattern having lower peak gain, whereas at higher frequencies such as 2.6 GHz and 3.4 GHz, the length required to produce resonance is smaller; therefore, the current is distributed on smaller lengths and mainly on one side (left or right) of the middle patch to produce radiation patterns with higher peak gains.

To validate this theory and understand the working mechanism of this reconfigurable antenna at different frequencies under different switching combinations/cases, the current distributions/surface currents at different frequencies for different cases/switching combinations are shown in Figs. 15–20 where the front side of the antenna is made bold, and back side is dimmed to make the picture understandable avoiding confusion.

It is obvious from these current distributions that at higher frequencies, the current is distributed only on smaller lengths (including top and bottom side) and mainly on one part/some parts (right, left,

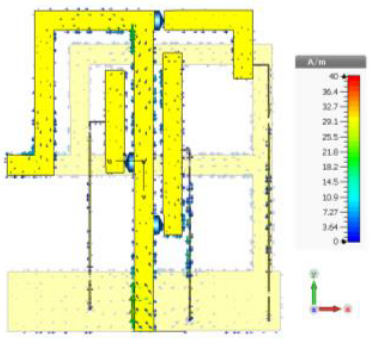

**Figure 15.** Surface current for case 1 (000) at 2.64 GHz.

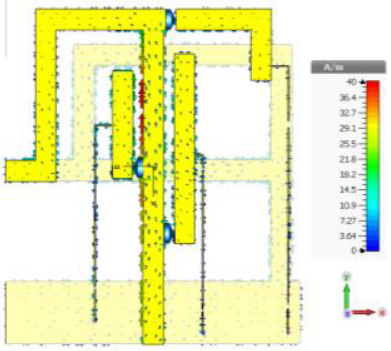

**Figure 16.** Surface current for case 2 (001) at 1.4 GHz.

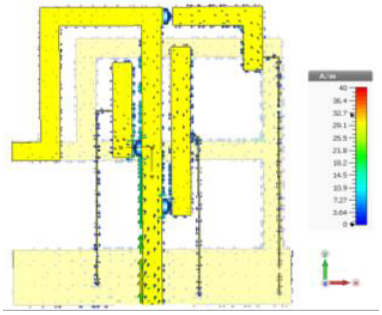

**Figure 17.** Surface current for case 3 (011) at 1.7 GHz.

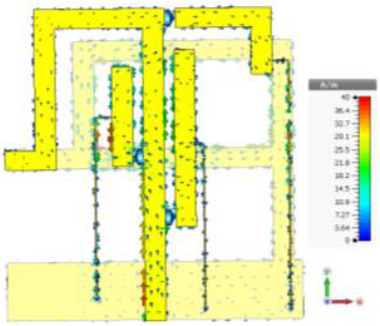

**Figure 18.** Surface current for case 5 (101) at 0.91 GHz.

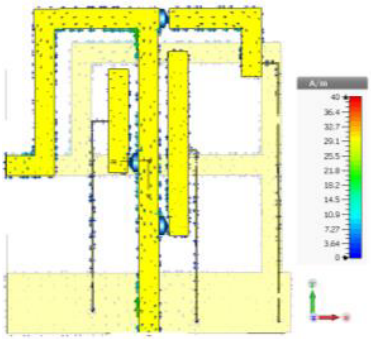

**Figure 19.** Surface current for case 6 (110) at 3.4 GHz.

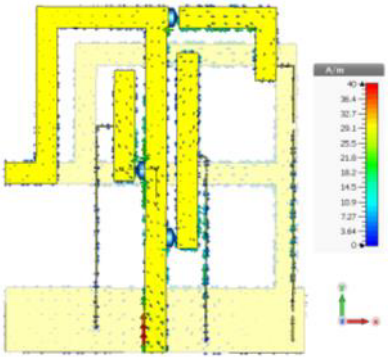

**Figure 20.** Surface current for case 7 (111) at 2.6 GHz.

upper portion, lower portion) of the antenna structure to produce relatively directive radiation pattern as evident from Figs. 15, 19, and 20, whereas at lower frequencies such as at 0.91 GHz, 1.4 GHz, and 1.7 GHz, the current is distributed on larger lengths of the patches (including top and bottom sides) of the antenna and on majority parts (right, left) of the antenna to produce radiation patterns with comparatively lower peak gains as shown in Figs. 16, 17 and 18. As shown in Fig. 18, the current is not only distributed on top and bottom sides of the antenna but also on both right and left hand sides in the bottom plane to produce the length of $\lambda/4$ corresponding to 0.91 GHz, having an omni-directional radiation pattern with lower peak gain.

## 6. CONCLUSION

A novel reconfigurable antenna design is presented in this paper. It operates in different LTE and GSM bands. Frequency reconfigurability is achieved with the help of three RF PIN diodes, and DC lines are inserted to control PIN diodes. A prototype of the proposed antenna is fabricated to verify the results. The theory behind the design is discussed, and the current distributions under different switching combinations are shown to validate the theory and the obtained results.

The radiation patterns prove that this antenna also exhibits pattern reconfigurability at different frequencies for different switching combinations. The proposed antenna has a great potential in becoming an integral part of future mobile communication.

## ACKNOWLEDGMENT

The work was supported in part by the Islamic University of Madinah, Saudi Arabia under Grant No. 11/B/1437 and in part by National Natural Science Foundation of China (Grant No. 61671349).

## REFERENCES


1. Haykin, S., "Cognitive radio: Brain-empowered wireless communications," *IEEE Journal on Selected Areas in Communications*, Vol. 23, No. 2, 201–220, 2005.
2. Aberle, J. T., S. H. Oh, D. T. Auckland, and S. D. Rogers, "Reconfigurable antennas for wireless devices," *IEEE Antennas Propag. Mag.*, Vol. 45, No. 6, 148–154, Dec. 2003.
3. Christodoulou, C. G., Y. Tawk, S. A. Lane, and S. R. Erwin, "Reconfigurable antennas for wireless and space applications," *Proc. IEEE*, Vol. 100, No. 7, 2250–2261, 2012.
4. Costantine, J., Y. Tawk, S. E. Barbin, and C. G. Christodoulou, "Reconfigurable antennas: Design and applications," *Proc. IEEE*, Vol. 103, No. 3, 424–437, Mar. 2015.
5. Haider, N., D. Caratelli, and A. G. Yarovoy, "Recent developments in reconfigurable and multiband antenna technology," *International Journal of Antennas and Propagation*, Vol. 2013, 1–14, 2013.
6. Yang, S., C. Zhang, H. K. Pan, A. E. fathy, and V. K. Nair, "Frequency-reconfigurable antennas for multiradio wireless platforms," *IEEE Antennas Microwave Mag.*, Vol. 10, No. 1, 66–83, Feb. 2009.
7. Anagnostou, D. E. and A. A. Gheethan, "Coplanar reconfigurable folded slot antenna without bias network for WLAN applications," *IEEE Antennas Wireless Propag. Lett.*, Vol. 8, 1057–1060, 2009.
8. Yassin, A. A., R. A. Saeed, R. A. Alsaqour, and R. A. Mokhtar, "Design of reconfigurable multiband microstrip patch antenna with a ground slot for WLAN & WiMax applications," *Inter. Journal of Applied Engineering Research*, Vol. 9, 6257–6266. Nov. 2014.
9. Tekin, I. and M. Knox, "Reconfigurable microstrip patch antenna for WLAN software defined radio applications," *Microw. Opt. Technol. Lett.*, Vol. 54, No. 3, 644–649, Mar. 2012.
10. Aftab, N., H. T. Chattha, Y. Jamal, A. Sharif, and Y. Huang, "Reconfigurable patch antenna for wireless applications," *2015 9th European Conference on Antennas and Propagation (EuCAP)*, 1–3, Apr. 13–17, 2015.
11. Anagnostou, D. E., M. T. Chryssomallis, B. D. Braaten, J. L. Ebel, and N. Sepúlveda, "Reconfigurable UWB antenna with RF-MEMS for on-demand WLAN rejection," *IEEE Trans. Antennas Propagat.*, Vol. 62, No. 2, 602–608, Feb. 2014.
12. Hinsz, L. and B. D. Braaten, "A frequency reconfigurable transmitter antenna with autonomous switching capabilities," *IEEE Trans. Antennas Propagat.*, Vol. 62, No. 7, 3809–3813, Jul. 2014.
13. Fallahpour, M., M. T. Ghasr, and R. Zoughi, "Miniaturized reconfigurable multiband antenna for multi-radio wireless communication," *IEEE Trans. Antennas Propagat.*, Vol. 62, No. 12, 6049–6059, Dec. 2014.
14. Jiang, Z. and F. Yang, "Reconfigurable sensing antennas integrated with thermal switches for wireless temperature monitoring," *IEEE Antennas Wireless Propag. Lett.*, Vol. 12, 914–917, 2013.
15. Khidre, A., K. F. Lee, F. Yang, and A. Z. Elsherbeni, "Circular polarization reconfigurable wideband E-shaped patch antenna for wireless applications," *IEEE Trans. Antennas Propagat.*, Vol. 61, No. 2, 960–964, Feb. 2013.
16. Kulkarni, A. N. and S. K. Sharma, "Frequency reconfigurable microstrip loop antenna covering LTE bands with MINO implementation and wideband microstrip slot antenna all for portable wireless dtv media player," *IEEE Trans. Antennas Propagat.*, Vol. 61, No. 2, 964–967, Feb. 2013.
17. Rajagopalan, H., J. M. Kovitz, and Y. R. Samii, "MEMS reconfigurable optimized E-shaped patch antenna design for cognitive radio," *IEEE Trans. Antennas Propagat.*, Vol. 62, No. 3, 1056–1064, Mar. 2014.
18. Zohur, A., H. Mopidevi, D. Rodrigo, M. Unlu, L. Jofre, and B. A. Cetiner, "RF MEMS reconfigurable two-band antenna," *IEEE Antennas Wireless Propag. Lett.*, Vol. 12, 72–75, 2013.
19. Boyle, K. R. and P. G. Steeneken, "A five-band reconfigurable PIFA for mobile phones," *IEEE Trans. Antennas Propagat.*, Vol. 55, No. 11, 3300–3309, Nov. 2007.
20. Lim, J. H., G. T. Back, Y. I. Ko, C. W. Song, and T. Y. Yun, "A reconfigurable PIFA using a switchable PIN-diode and a fine-tuning varactor for USPCS/WCDMA/m-WiMAX/WLAN," *IEEE Trans. Antennas Propagat.*, Vol. 58, No. 7, 2404–2411, Jul. 2007.

21. Elfergani, I. T. E., T. Sadeghpour, R. A. Abd-Alhameed, A. S. Hussaini, J. M. Noras, S. M. R. Jones, and J. Rodriguez, "Reconfigurable antenna design for mobile handsets including harmonic radiation measurements," *IET Microw. Antennas Propag.*, Vol. 6, No. 9, 990–999, 2012.
22. Wang, B. Z., S. Xiao, and J. Wang, "Reconfigurable patch antenna design for wideband wireless communication systems," *IET Microw. Antennas Propag.*, Vol. 1, No. 2, 414–419, Apr. 2007.
23. Ali, M. A. M., "Design and analysis of adaptive and reconfigurable antennas for wireless communication," Doctoral Dissertation, University of Central Florida, Orlando, USA, 2004.
24. Xiao, S., B. Z. Wang, X. S. Yang, and G. Wang, "A novel frequency reconfigurable patch antenna," *Microw. Opt. Technol. Lett.*, Vol. 36, 295–297, Feb. 2003.
25. Nikolaou, S., R. Bairavasubramanian, and C. Lugo, "Pattern and frequency reconfigurable annular slot antenna using pin diodes," *IEEE Trans. Antennas Propagat.*, Vol. 54, No. 2, 439–448, 2006.
26. Sathi, V., N. Ehtheshami, and J. Nourinia, "Optically tuned frequency reconfigurable microstrip antenna," *IEEE Antennas Wireless Propag. Lett.*, Vol. 11, 1018–1020, 2012.
27. Pendharker, S., R. K. Shevgaonkar, and A. N. Chandorkar, "Optically controlled frequency-reconfigurable microstrip antenna with low photoconductivity," *IEEE Antennas Wireless Propag. Lett.*, Vol. 13, 99–102, 2014.
28. Liu, L. and R. J. Langley, "Liquid crystal tunable microstrip patch antenna," *IET Electron. Lett.*, Vol. 44, No. 20, 1179–1180, 2008.
29. Rodrigo, D., L. Jofre, and B. Cetiner, "Circular beam-steering reconfigurable antenna with liquid metal parasitics," *IEEE Trans. Antennas Propagat.*, Vol. 60, No. 4, 1796–1802, 2012.
30. Constantine, J., Y, Tawk, J. Woodland, N. Floam, and C. G. Christodoulou, "Reconfigurable antenna system with a movable ground plane for cognitive radio," *IET Microw. Antennas Propag.*, Vol. 8, No. 11, 858–863, 2014.
31. Boukarkar, A., X. Q. Lin, and Y. Jiang, "A new reconfigurable multi-band monopole antenna for different wireless applications," *2015 IEEE International Conference on Communication Software and Networks (ICCSN)*, 6–7, Chengdu, China, 2015.
32. Yadav, A. M., C. J. Panagamuwa, and R. D. Seager, "A miniature reconfigurable printed monopole antenna for WLAN/WiMAX and LTE communication bands," *2012 Loughborough Antennas & Propagation Conference (LAPC),* 1–4, 2012.
33. Iddi, H. U., M. R. Kamarudin, T. A. Rahman, and R. Dewan, "Reconfigurable monopole antenna for WLAN/WiMAX applications," *PIERS Proceedings*, 1048–1051, Taipei, Mar. 25–28, 2013.
34. Ali, M. M. M., A. M. Azmy, and O. M. Haraz, "Design and implementation of reconfigurable quad-band microstrip antenna for MIMO wireless communication applications," *2014 31st National Radio Science Conference (NRSC)*, Cairo, Egypt, April 28–30, 2014.
35. Minh, P. T., T. T. Thao, N. T. Duc, and V. V. Yem, "A novel multiband frequency reconfigurable PIFA antenna," *2016 International Conference on Advanced Technologies for Communications (ATC)*, 7–12, 2016.
36. Al-Alaa, M. A., H. A. Elsadek, E. A. Abdallah, and E. A. Hashish, "PIFA frequency reconfigurable antenna," *2014 IEEE Antennas and Propagation Society International Symposium (APSURS*I), 1256–1257, 2014.
37. Mak, A. C. K., C. R. Rowell, R. D. Murch, and C. L. Mak, "Reconfigurable multiband antenna designs for wireless communication devices," *IEEE Trans. Antennas Propagat.*, Vol. 55, No. 7, 1919–1928, 2007.
38. Pozar, D. M., *Microwave Engineering*, 4th edition, John Wiley & Sons, 2012.
39. Balanis, C. A., *Antenna Theory: Analysis and Design*, 3rd edition, John Wiley & Sons, 2005.